

Porosity Reduction in Large-Format Additive Manufacturing of Fiber-Reinforced Composites via Elongational Screw Design

Aywan Das^a and Chad E. Duty^{a,b}

^a*University of Tennessee, Knoxville – Department of Mechanical and Aerospace Engineering,
1512 Middle Dr, 414 Dougherty Engineering Building, Knoxville, TN 37996, USA*

^b*Manufacturing Demonstration Facility, Oak Ridge National Laboratory, 2370 Cherahala Blvd.,
Knoxville, TN 37932, USA*

^a Aywan Das, *E-mail address:* adas16@vols.utk.edu

^b Chad E. Duty, *E-mail address:* cduty@utk.edu

ABSTRACT

As Large-Format Additive Manufacturing (LFAM) advances toward structurally demanding applications, internal porosity in extruded fiber-reinforced beads (typically 4–10% by volume) remains a limiting factor for mechanical performance. This study investigates porosity reduction using a single-screw lab-scale extrusion system (Randcastle Microtruder Model RCP-1000) to evaluate the effects of nozzle diameter (6.35 mm), temperature (205–250 °C), and screw speed (15–105 rpm) on flow rate, shear rate, viscosity, and porosity in 40 wt% glass fiber-filled ABS. Consistent bead collection was ensured using a conveyor belt, and Archimedes density analysis was applied to quantify internal voids. Ongoing work compares a conventional screw and a patented Spiral Fluted Elongational Mixer (SFEM) screw from Randcastle Systems to assess the impact of elongational mixing on porosity and melt homogeneity. This study aims to establish extrusion parameter–porosity relationships and inform design decisions for next-generation LFAM systems using highly filled reinforced polymer composites.

1. INTRODUCTION

One of the earliest LFAM demonstrations was ORNL’s Big Area Additive Manufacturing (BAAM) platform, which uses pellet-fed single-screw extrusion [1]. ORNL subsequently extended LFAM from a gantry system to robot-mounted deposition. The combination of low-cost pellet feed and flexible robotics has accelerated adoption due to high throughput and straightforward integration and is now widely used across research and industry [2], [3]. Nevertheless, porosity remains one of the most critical defects in extrusion-based fabrication of fiber-reinforced thermoplastics. Even at low levels, voids interrupt stress transfer between fiber and matrix, acting as nucleation sites for cracks and lowering structural reliability. Studies have shown that pores accelerate fatigue crack initiation and growth by intensifying local stress and strain concentrations [4], [5]. In carbon fiber laminates, increased void content directly reduces interlaminar shear strength and fracture toughness [6], while in chopped-fiber thermoplastics porosity undermines fiber wetting and increases the chance of fiber pullout [7]. At the microstructural level, voids can trigger crazing and fiber–matrix debonding, promoting crack growth and accelerating local failure in composites [8]. Figure 1 shows an example of porosity observed in an extruded sample, where 18.4% void content was measured [9]. For these reasons, minimizing porosity is essential to achieve consistent strength, stiffness, and fatigue performance in LFAM.

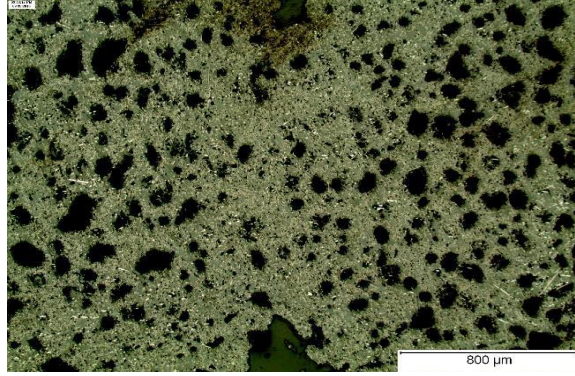


Figure 1: Porosity in an extruded sample: 18.4% Porosity [9]

The impact of porosity on mechanical behavior has been widely reported. Hakim et al. showed that interlaminar fracture toughness and fatigue life decrease sharply when porosity exceeds 3–5% [6]. Xu et al. demonstrated that even small pores located near the surface strongly magnify local strain fields, driving early fatigue crack initiation [4]. Serial sectioning and computed tomography confirm that pores are not uniformly distributed but cluster around fiber ends or inter-bead boundaries [10]. Porosity promotes anisotropy because voids tend to align along the extrusion direction, leading to direction-dependent properties [7]. Fiber–void interactions further exacerbate property degradation. Sayah and Smith [11] reported that regions of higher void volume fraction in LFAM beads correspond to reduced fiber orientation and lower fiber volume fraction, highlighting the coupled influence of fiber distribution and porosity on composite performance. Thus, porosity reduction is not only about densification but also about preserving fiber alignment and effective load transfer.

The formation of voids during extrusion is driven by several mechanisms. Moisture absorbed in hydrophilic feedstocks evolves as vapor during heating, forming bubbles that expand as pressure decreases near the die exit [12]. Trapped ambient gases within the interstitial spaces of loosely packed pellets can be incorporated into the melt during feeding. Dissolved gases from prior pelletization may nucleate and expand under shear and pressure drop when the pressure gradient along the screw channel decreases. Additionally, local thermal degradation of the polymer matrix can release gaseous byproducts when temperature profiles exceed safe limits. Finally, cavitation phenomena associated with long fibers accelerating through the nozzle can leave voids trailing the fiber ends, correlating porosity with shear rate and fiber length. These mechanisms collectively result in void contents ranging from 4–10% in typical fiber-reinforced LFAM beads [13].

Recent work has shown that screw geometry is a powerful lever to reduce voids. The spiral fluted elongational mixing (SFEM) screw introduces strong elongational flow and recirculation (Figure 2), which not only disperses fibers more effectively but also have decompression zones where gases can be released [14]. When paired with venting ports in the barrel, these screws allow gases to escape before the melt is recompressed. This approach builds on earlier studies of vented extrusion, where devolatilization under shear and vacuum was found to enhance gas removal compared to conventional strand-based methods [15]. For fiber-reinforced composites, the combination of elongational flow and venting provides a practical path toward denser, more reliable extrudates.

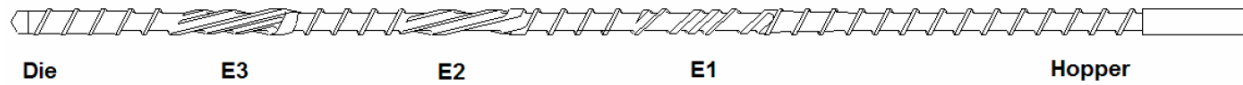


Figure 2: Elongator screw with three SFEM elements developed by Randcastle Extrusion Systems [16]

The goal of this work is to evaluate porosity reduction in glass-fiber-reinforced ABS extruded using two set of screws: a conventional two-stage screw and an SFEM screw. SFEM with venting capability were tested across a range of screw speeds. Porosity levels were quantified by the different density methods, providing new insight into how screw design and venting influence the quality of extruded fiber composites.

2. BACKGROUND

2.1 Advances in Screw Design

Conventional single-screw geometries rely primarily on shear-dominated flow, where the material is conveyed along helical channels with limited opportunities for distributive mixing. While adequate for neat polymers, these designs are less effective for fiber-filled composites where uniform dispersion, gas removal, and fiber wetting are critical. Poor mixing leaves voids unbroken, and without decompression zones, conventional screws cannot efficiently evacuate gases and any open vent risks melt blowout due to pressurization. Figure 3 presents a side-by-side comparison of the screw designs.

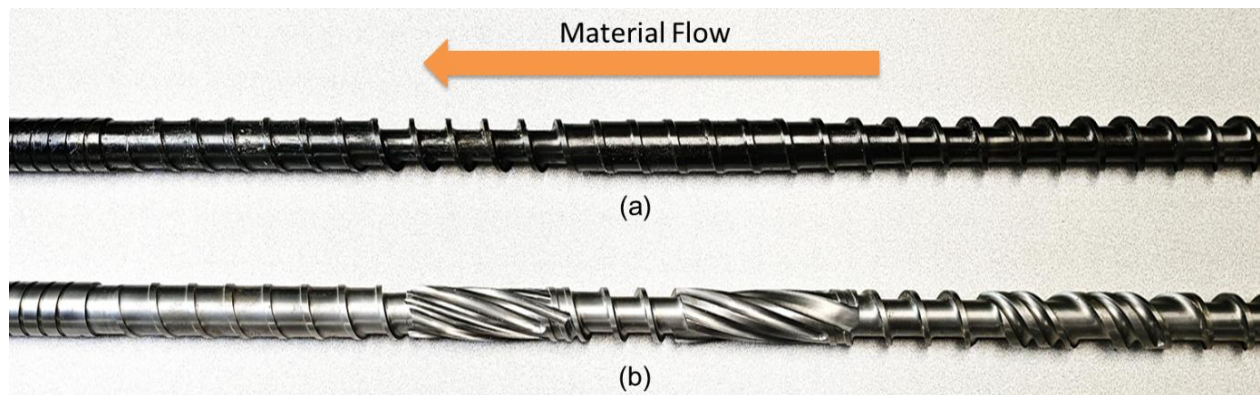


Figure 3: Side by side screw comparison: (a) Conventional two-stage screw and (b) SFEM screw

Elongational screws represent a significant departure from conventional two-stage shear-driven screws. In the SFEM design which is shown in Figure 4, material is conveyed forward into spiral channels (C1, C2, C3), where it experiences elongational deformation rather than primarily shear. As the polymer melt enters each channel, it is stretched longitudinally and redistributed by recirculation loops along the screw axis. This repeated stretching and redirection ensures uniform dispersive and distributive mixing [16], [17].

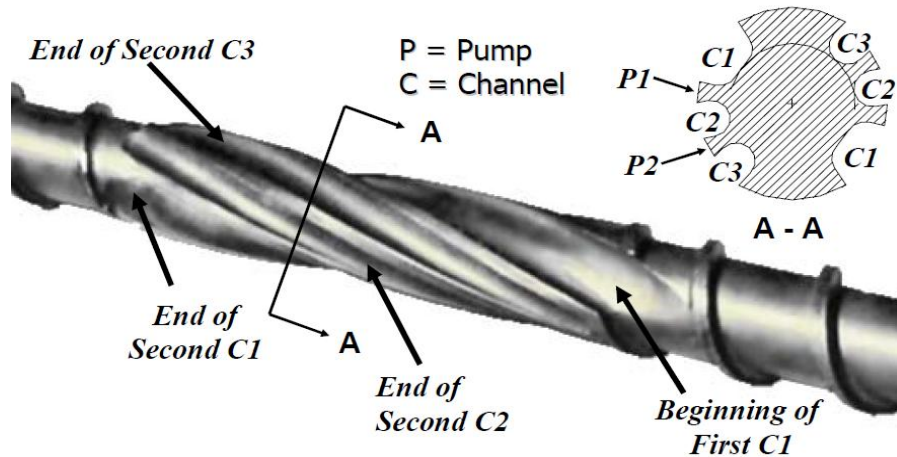


Figure 4: Elongator screw from Randcastle extrusion system [18]

The open-ended channel geometry reduces flow resistance, allowing smoother material transport with less pressure buildup. This not only minimizes shear heating but also provides low-pressure regions that facilitate the migration and escape of entrapped gases when combined with venting ports. By preventing back-mixing and maintaining forward material progression, elongational screws reduce the likelihood of bubbles re-entering the melt. The result is improved devolatilization and significantly lower porosity in extruded composites, enhancing fiber wetting, matrix densification, and mechanical reliability in. The design also promotes thin-film flow along flute surfaces, exposing a larger melt area to vent ports for degassing. Additionally, elongational mixing reduces thermal degradation by minimizing localized shear heating compared to high-shear conventional designs.

2.2 Venting in Extrusion

A distinctive feature of the SFEM screw is its integrated venting mechanism. By incorporating two decompression zones followed by two atmospheric vents, the screw geometry ensures that system pressure drops locally, allowing dissolved and entrained gases to escape without melt ejection. This design mimics the gas-removal strategies long used in vented twin-screw systems but adapted for single-screw LFAM platforms where weight and complexity must remain low.

Vacuum venting provides an even stronger driving force for degassing by reducing the pressure in the vent section, which promotes bubble growth and release. For venting to be effective, the screw must create conditions where the polymer melt forms a stable film rather than a pressurized bulk flow. In SFEM screws, the spiral flutes naturally spread the melt into thin layers as it passes the vent, dramatically increasing interfacial area for gas release. After venting, the melt is recompressed to seal the flow and restore pressure for downstream pumping. This thin-film devolatilization mechanism is critical because it minimizes the likelihood of gases being carried further into the extrudate. As a result, the combination of decompression zones, venting ports, and elongational mixing allows the SFEM screw to achieve significantly lower porosity than conventional shear-based screws. An exploded view of the entire Randcastle Microtruder is shown in the Figure 5.

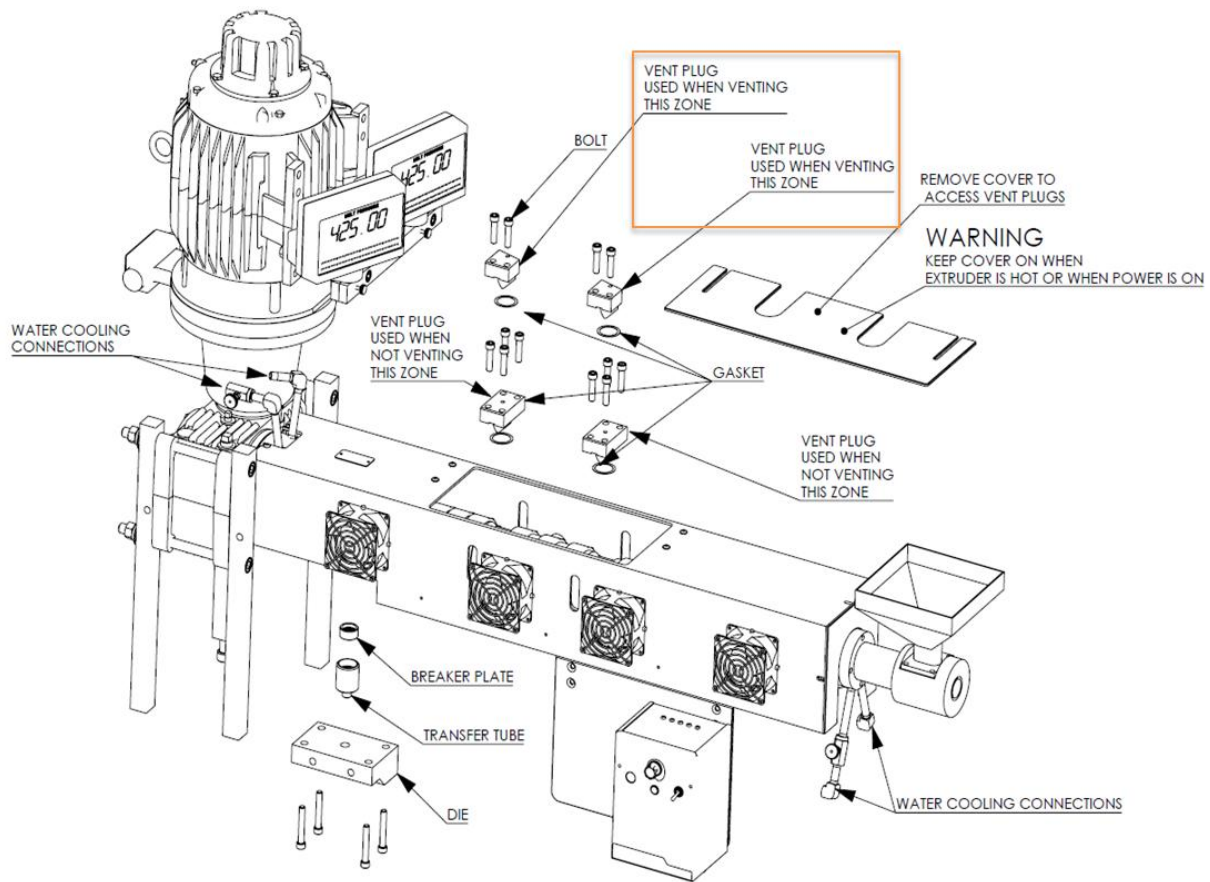


Figure 5: Exploded view of the Randcastle Microtruder Model RCP-1000 [19]

2.3 Measurement Techniques for Porosity

Porosity quantification requires distinguishing between bulk, skeletal, and true densities (Figure 6). Bulk density is measured from mass and external volume, capturing both solid and void content. Skeletal density, obtained via helium pycnometry, excludes open porosity since helium penetrates only closed pore-free solid volume [20]. True density refers to the pore-free density of the polymer–fiber mixture, determined from reference materials or injection-molded samples. Porosity is then calculated by comparing experimental bulk density to the true density.



Figure 6: Understanding different density types

The Archimedes method is the most common bulk technique, where density is determined by immersion in fluid. However, it is sensitive to surface roughness, open pores, and air entrapment [21]. Vacuum-assisted Archimedes reduces this error by degassing samples during immersion. Helium pycnometry, in contrast, provides accurate skeletal density because helium atoms penetrate small, closed pores and do not adsorb to the material [20].

Micro-computed tomography (μ CT) is a powerful non-destructive method to visualize and quantify porosity in LFAM composites, providing three-dimensional information on void size, morphology, and spatial distribution, and has revealed skin-core porosity gradients and correlations between void-rich regions and reduced fiber alignment [10], [11]. However, μ CT was not selected in this study due to its limited resolution-volume trade-off for large beads, long scanning times, and difficulty in capturing microporosity relevant to extrusion trials. Instead, a combination of Archimedes, vacuum Archimedes, and helium pycnometry was employed, offering a practical, repeatable, and accurate approach for evaluating porosity across multiple extrusion runs, while μ CT will be considered in future work as a complementary validation tool.

3. EXPERIMENTAL SETUP

3.1 Extrusion System

Experiments were performed using a Randcastle Microtruder RCP-1000 single-screw extrusion platform which is shown in Figure 7. Two screw designs were evaluated: a conventional screw and a SFEM screw incorporating a decompression region and venting port. The system consists of a 24:1 L/D barrel, four heating zones, a die zone, and a 0.25 in (6.35 mm) diameter nozzle. The extruder is horizontally oriented and supported by a gearbox and motor assembly capable of operating up to 115 rpm.

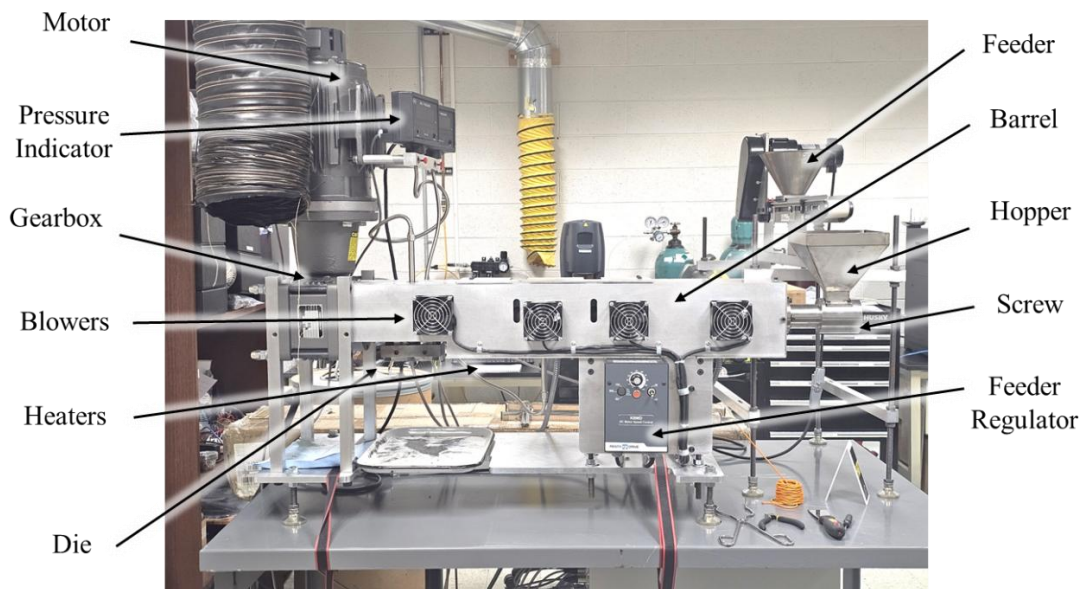


Figure 7: Randcastle extrusion system whole setup

The die assembly includes a breaker plate and transfer tube, while pressure safety is ensured by a rupture disc and a vented barrel section for SFEM operation. Power is supplied to five independent heaters (four barrel zones and one die zone), with real-time monitoring through a digital control panel.

Traditional extrusion setups typically produce a pile of extrudate, which is not suitable for consistent material characterization. To address this, a conveyor belt system was integrated downstream of the nozzle. The conveyor provided controlled deposition of material into straight, uniform beads of consistent thickness which is shown in Figure 8. This enabled reliable specimen preparation for density and porosity testing. The conveyor could also be adjusted or scaled to accommodate different extrusion speeds and material types, ensuring flexibility across the test matrix.

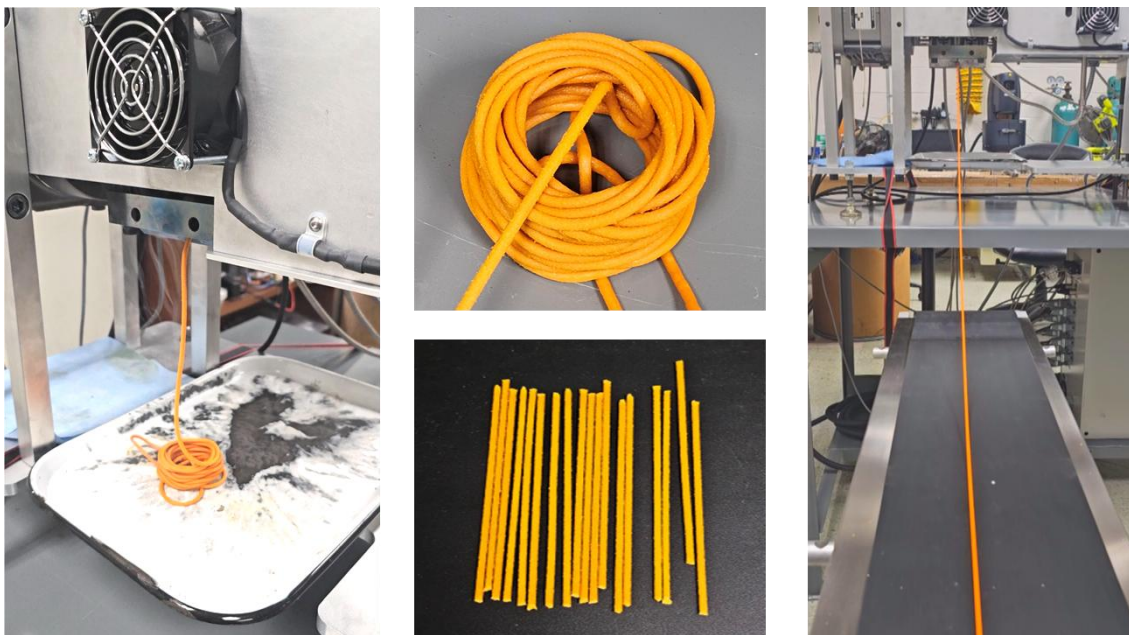


Figure 8: Use of conveyor belt to obtain flat, straight, and uniform extruded beads for consistent material characterization

3.2 Materials

The feedstock used was 40 wt% glass fiber-reinforced ABS pellets (Techmer PM, TN, USA). Pellets were stored in sealed containers and dried at 85 °C for four hours prior to extrusion to minimize moisture-driven porosity.

3.3 Processing Parameters

Extrusion tests were carried out under the following baseline thermal profile:

- Zone 1: 400 °F
- Zone 2: 450 °F

- Zone 3: 475 °F
- Zone 4: 485 °F
- Die: 480 °F

Different screw speeds were selected ranging from 20 to 100 rpm to study the effect of shear rate and residence time on porosity. Extrusion trials were conducted under starve-fed conditions using a gravity hopper. For vented trials, the barrel vent ports were left open to atmosphere; for comparison, the same runs were performed with vents closed.

3.4 Density and Porosity Measurement

Porosity quantification was performed using three complementary methods shown in Figure 9, each capturing different aspects of void content in fiber-reinforced composites.

1. **Archimedes Method:** Bulk density was determined by measuring the buoyant force on a specimen immersed in deionized water using Meter Toledo equipment. This simple and widely used method is effective for estimating overall porosity but can underestimate void content if closed pores trap air, preventing fluid infiltration.
2. **Vacuum-Assisted Archimedes Method:** To mitigate the limitations of the conventional Archimedes approach, samples were subjected to vacuum prior to immersion. This process removes air trapped in surface-connected voids and improves wetting of the porous network, yielding more reliable results in fiber-filled systems where microvoids are often located around fiber–matrix interfaces.

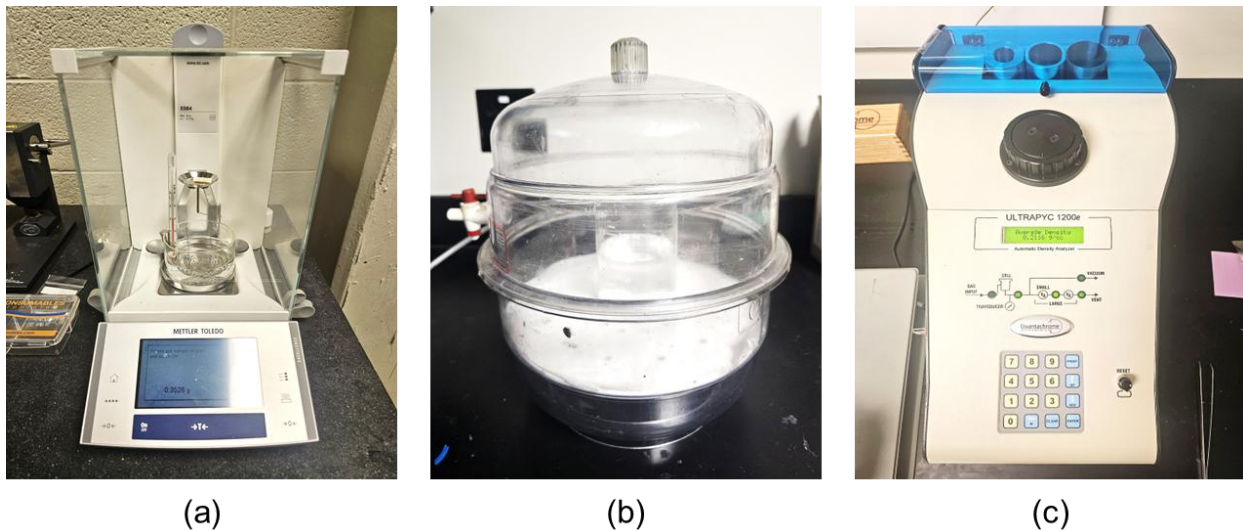


Figure 9: Different density measurement methods: (a) Archimedes method, (b) Vacuum-assisted Archimedes method, and (c) Helium Pycnometry

3. **Helium Pycnometry:** True skeletal density (ρ_{skeletal}) was obtained using helium pycnometry, which allows helium atoms to penetrate into fine closed pores on the order of microns. By comparing skeletal density with bulk density, the closed-void fraction can be distinguished from open porosity. Pycnometry is particularly advantageous in fiber composites where porosity exists both as dispersed intra-bead voids and interfacial cavities around fibers.

Porosity was calculated as:

$$\text{porosity} = 100\left(1 - \frac{\rho}{\rho_0}\right)$$

Where, ρ = experimental density
 ρ_0 = true density measured via injection-molded fiber-filled ABS samples, assumed to represent near-zero porosity.

Together, these methods provide a hierarchical view of porosity: Archimedes for gross density changes, vacuum-assisted Archimedes for semi-closed void correction, and helium pycnometry for closed voids.

3.5 Safety and Operational Considerations

Operation of the single-screw extruder requires careful safety management:

- Pressure control: The barrel is equipped with a rupture disc to prevent catastrophic failure in the event of over-pressurization.
- Screw overload: Continuous monitoring of the ammeter prevents operation under frozen or overfilled conditions that can damage the screw.
- Venting hazards: The vented section may release hot gases and entrained melt; the vent port must be covered when active to prevent operator injury.

4. RESULTS AND DISCUSSION

4.1 Comparison of Density Measurement Methods

Figure 10 shows the porosity values obtained using three techniques: regular Archimedes, vacuum-assisted Archimedes, and helium pycnometry. At 20 rpm, Archimedes gave an apparent porosity of ~3–4%, while vacuum Archimedes indicated ~6–7%, and helium pycnometry ~8–9%. This trend held across all speeds: Archimedes consistently underestimated porosity, vacuum-assisted immersion corrected part of the error, and helium pycnometry gave the most reliable and stable values. At 20 rpm, for example, Archimedes measured nearly 5 percentage points lower than helium pycnometry, which would make screw design effects appear smaller than they actually are.

At higher speeds (higher than 60 rpm), porosity decreased for all methods, but the relative ranking remained. For example, at 100 rpm with the SFEM screw, porosity was ~2% by Archimedes, ~4–5% by vacuum Archimedes, and ~6% by helium pycnometry. These results align with prior studies where liquid immersion tests were found to miss closed porosity, while gas-based methods captured it accurately.

Porosity vs Reg Screw RPM for
Different Density Measurement Methods

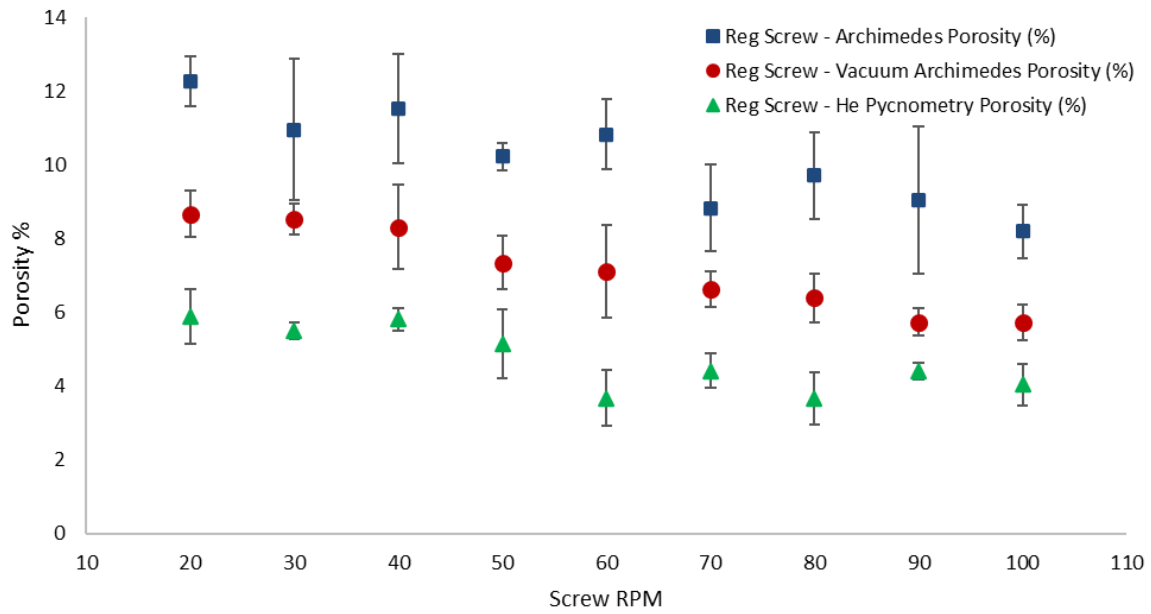


Figure 10: Comparison of different density measurement methods

4.2 Effect of Screw Design on Porosity

Porosity vs Screw RPM in terms of Screw Geometry

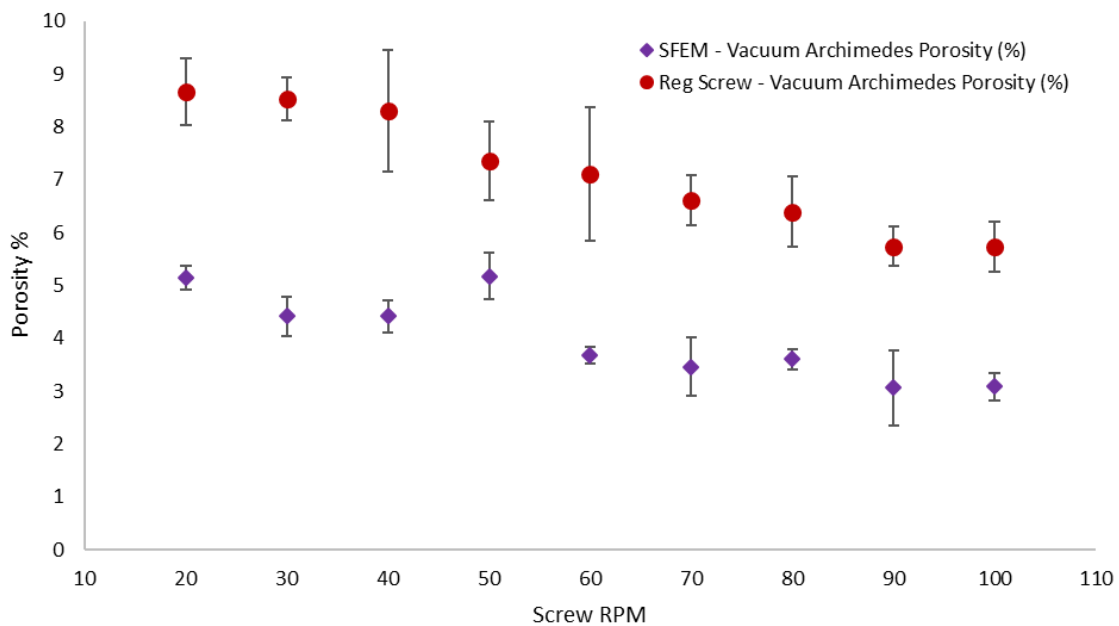


Figure 11: Comparison of two screws using the vacuum Archimedes method

As shown in Figure 11, the SFEM screw consistently reduced porosity compared to the conventional screw. At 20 rpm, the conventional screw showed ~9% porosity (vacuum Archimedes) versus ~6% for the SFEM screw. At 100 rpm, both screws improved due to higher shear, but SFEM maintained a 2–3% advantage. Across all speeds, the average porosity reduction achieved by SFEM was 2–3.5%.

The improvement can be traced to the screw geometry. The spiral flutes promote elongational flow, which stretches and ruptures bubbles, while the integrated venting zones provide pressure drops for gas escape. The conventional screw lacked such decompression zones, so opening a vent would risk melt blowout rather than controlled degassing.

4.3 Effect of Screw Speed

Increasing screw speed was found to decrease porosity for both the conventional and SFEM screws. At low speeds (i.e., 20 rpm), porosity levels were highest because the polymer melt remained inside the extruder longer. This extended residence time allowed volatiles, residual moisture, and trapped air to nucleate and grow into bubbles before the material exited. In this regime, the venting mechanism of the SFEM screw played a critical role in removing gases before solidification, leading to noticeably lower porosity compared to the conventional screw.

As screw speed increased to 60 rpm, porosity progressively decreased. The reduction is attributed to two factors: (i) improved mixing and dispersive action at higher shear rates, which breaks up bubbles and enhances fiber wetting, and (ii) faster material throughput, which reduces residence time and thus limits the opportunity for bubbles to form and coalesce. The impact of screw speed was most prominent at lower rpm, where porosity differences between the two screws were largest. At higher rpm, both screws benefited from faster throughput, but the SFEM screw consistently maintained a 2–3% porosity advantage due to its elongational mixing and venting capability.

4.4 Implications for Fiber-Reinforced Composites

The results demonstrate that screw geometry and venting are critical for porosity control in fiber-filled extrusion. Lower porosity directly translates into improved mechanical reliability, as voids are known to reduce interlaminar shear strength, stiffness, and fatigue life. In LFAM, where bead-scale porosity of 4–10% is common, the SFEM screw provides a viable strategy to push porosity toward the lower end of this range. The measurement comparison also highlights a methodological lesson: Archimedes alone is insufficient for reliable porosity assessment, and vacuum-assisted Archimedes combined with helium pycnometry offers a more accurate and practical approach.

5. CONCLUSION AND FUTURE WORK

This study investigated porosity reduction in single-screw extrusion of fiber-reinforced ABS composites by comparing a conventional screw to a SFEM screw with venting capability. The following conclusions can be drawn:

1. Screw geometry significantly impacts porosity. The SFEM screw consistently reduced porosity by 2–3.5% compared to the conventional screw across all processing speeds. This improvement was attributed to the elongational mixing action, which promotes ligament thinning and gas release, and to the venting section, which enables effective devolatilization.
2. Screw speed influences void content. Increasing screw speed decreased porosity for both screw types. At low speeds, long residence times promoted bubble formation, making venting particularly important. At higher speeds, improved mixing and shorter residence times reduced porosity, although the SFEM screw maintained an inherent advantage.
3. Porosity measurement methods capture different aspects of void content. Regular Archimedes underestimated porosity because of trapped air, while vacuum-assisted Archimedes and helium pycnometry provided more accurate results. Helium pycnometry was the most consistent, but vacuum Archimedes offered a practical compromise for repeated extrusion trials.
4. Mechanical implications of porosity reduction are significant. Lower void fractions improve fiber–matrix wetting, reduce fiber pullout, and minimize stress concentrators that serve as fatigue crack initiation sites. The observed porosity reduction with the SFEM screw therefore translates to improved strength, stiffness, and durability of fiber-reinforced composites.

Future Work

Building on these findings, several directions are recommended:

- Performing mechanical testing (tensile, flexural, and fatigue) on extrudates to directly correlate porosity reduction with property improvements.
- Conducting microscopy and μ CT imaging to validate pore morphology and distribution trends observed from density measurements.
- Studying how processing conditions and screw geometry influence fiber length and orientation, with a focus on fiber length distribution along the screwline in conventional two-stage versus elongational vented screws, to understand how design impacts fiber breakage and retention.
- Combining vented screws with vacuum-assisted hopper systems, as demonstrated in recent LFAM work, may further reduce porosity below 2% and approach injection-molded quality.

Overall, the results highlight that advanced screw geometries such as SFEM, when combined with venting, are a promising pathway to address one of the most critical barriers in extrusion-based additive manufacturing: the control of porosity in fiber-reinforced thermoplastic composites.

6. REFERENCES

- [1] C. E. Duty and others, “Structure and mechanical behavior of Big Area Additive Manufacturing (BAAM) materials,” *Rapid Prototyp J*, vol. 23, no. 1, pp. 181–189, 2017, doi: 10.1108/RPJ-12-2015-0183.
- [2] A. Das, “Development of a Large Format Additive Manufacturing System Based on an Off-The-Self Pellet Extruder,” MS Thesis, University of South Carolina, Columbia, 2024. Accessed: Sep. 20, 2025. [Online]. Available: <https://scholarcommons.sc.edu/etd>
- [3] A. Das and W. De Backer, “Multi-axis Pellet Based Extrusion for Large Format Additive Manufacturing,” in *The Composites and Advanced Materials Expo*, 2023, pp. 497–514. doi: 10.33599/nasampe/c.23.0090.
- [4] Z. Xu, W. Wen, and T. Zhai, “Effects of pore position in depth on stress/strain concentration and fatigue crack initiation,” in *Metallurgical and Materials Transactions A: Physical Metallurgy and Materials Science*, Aug. 2012, pp. 2763–2770. doi: 10.1007/s11661-011-0947-x.
- [5] M. Mehdikhani, L. Gorbatikh, I. Verpoest, and S. V. Lomov, “Voids in fiber-reinforced polymer composites: A review on their formation, characteristics, and effects on mechanical performance,” May 01, 2019, *SAGE Publications Ltd*. doi: 10.1177/0021998318772152.
- [6] I. A. Hakim *et al.*, “Porosity Effects on Interlaminar Fracture Behavior in Carbon Fiber-Reinforced Polymer Composites,” *Materials Sciences and Applications*, vol. 8, no. 2, pp. 170–187, Feb. 2017, doi: 10.4236/MSA.2017.82011.
- [7] V. Kumar *et al.*, “High-performance molded composites using additively manufactured preforms with controlled fiber and pore morphology,” *Addit Manuf*, vol. 37, p. 101733, Jan. 2021, doi: 10.1016/J.ADDMA.2020.101733.
- [8] K. A. Chowdhury, R. Talreja, and A. A. Benzerga, “Effects of Manufacturing-Induced Voids on Local Failure in Polymer-Based Composites,” 2008, doi: 10.1115/1.2841529.
- [9] F. L. Mattingly, A. Franc, V. Kunc, and C. Duty, “CHARACTERIZING INTERNAL POROSITY OF 3D-PRINTED FIBER REINFORCED MATERIALS,” in *Solid Freeform Fabrication Symposium*, Austin, 2021.
- [10] A. G. Stamopoulos, K. I. Tserpes, P. Prucha, and D. Vavrik, “Evaluation of porosity effects on the mechanical properties of carbon fiber-reinforced plastic unidirectional laminates by X-ray computed tomography and mechanical testing,” *J Compos Mater*, vol. 50, no. 15, pp. 2087–2098, Jun. 2016, doi: 10.1177/0021998315602049;SUBPAGE:STRING:ABSTRACT;WEBSITE:WEBSITE:SAGE;REQUESTEDJOURNAL:JOURNAL:JCMA;WGROUPE:STRING:PUBLICATION.

- [11] N. Sayah and D. E. Smith, “Fiber and Void Property Correlation within Bead Microstructure of Large Area Additive Manufacturing Polymer Composites,” in *TWENTY-THIRD INTERNATIONAL CONFERENCE ON COMPOSITE MATERIALS (ICCM23)*, 2023. [Online]. Available: <https://www.researchgate.net/publication/381796340>
- [12] Z. A. Mohd Ishak and J. P. Berry, “Effect of moisture absorption on the dynamic mechanical properties of short carbon fiber reinforced nylon 6, 6,” *Polym Compos*, vol. 15, no. 3, pp. 223–230, Jun. 1994, doi: 10.1002/PC.750150308;CTYPE:STRING:JOURNAL.
- [13] F. Mattingly, V. Kumar, K. Chawla, W. Bras, V. Kunc, and C. Duty, “Vacuum-assisted extrusion to reduce internal porosity in large-format additive manufacturing,” *Addit Manuf*, vol. 97, Jan. 2025, doi: 10.1016/j.addma.2024.104612.
- [14] K. Luker, “NOVEL SINGLE SCREW ELONGATIONAL COMPOUNDER FOR THERMALLY SENSITIVE MATERIALS.”
- [15] A. Tukachinsky, Y. Talmon, and Z. Tadmor, “Foam-enhanced devolatilization of polystyrene melt in a vented extruder,” *AIChE Journal*, vol. 40, no. 4, pp. 670–675, 1994, doi: 10.1002/AIC.690400410.
- [16] K. Luker and T. M. Cunningham, “INVESTIGATION INTO A HIGH OUTPUT POLYPROPYLENE SCREW AND ITS MIXING MECHANISM.”
- [17] K. Luker, “Single Screw Elongational Mixing Developments For Continuous Mixing Applications.”
- [18] K. Luker and M. E. Reedy, “THE DEVELOPMENT OF A NEW ELONGATION MIXING SCREW FOR FOAM AND ITS ADVANTAGES FOR FOAMING PLASTICS.” [Online]. Available: http://www.extrusiontechnicalservices.com/site_info.
- [19] K. Luker, “MICROTRUDER MANUAL,” 2015. Accessed: Aug. 08, 2024. [Online]. Available: www.randcastle.com
- [20] F. J. Semel and D. A. Lados, “Porosity analysis of PM materials by helium pycnometry,” *Powder Metallurgy*, vol. 49, no. 2, pp. 173–182, Jun. 2006, doi: 10.1179/174329006X95347.
- [21] T. de Terris *et al.*, “Optimization and comparison of porosity rate measurement methods of Selective Laser Melted metallic parts,” *Addit Manuf*, vol. 28, pp. 802–813, Aug. 2019, doi: 10.1016/j.addma.2019.05.035.

Acknowledgements

This work was supported by the National Science Foundation under Grant No. 2055529. The feedstock materials used in this research were supplied by Techmer PM, Clinton, TN, USA.